ISSN 0016-7932, Geomagnetism and Aeronomy, 2023, Vol. 63, No. 3, pp. 239–247. © Pleiades Publishing, Ltd., 2023.
Russian Text © The Author(s), 2023, published in Geomagnetizm i Aeronomiya, 2023, Vol. 63, No. 3, pp. 275–283.

Large-Scale Disturbances of the Solar Wind According to Spacecraft Radio Transmission Data from the Mars Express and Local Measurements on the Wind Spacecraft

A. I. Efimov[a], *, V. M. Smirnov[a], I. V. Chashei[b], and A. S. Nabatov[a]

[a] *Fryazinsky Branch of Kotelnikov Institute of Radio Engineering and Electronics, Russian Academy of Sciences (FIRE RAS), Fryazino, Moscow oblast, 141190 Russia*

[b] *Lebedev Physical Institute, Russian Academy of Sciences, Moscow, 119991 Russia*

**e-mail: efimov@ms.ire.rssi.ru*

Received November 18, 2022; revised January 11, 2023; accepted January 26, 2023

Abstract—The results of experiments on radio sounding of near the Sun plasma by the signals of the Mars Express Mars satellite are presented. In the region of heliocentric distances of the proximate point of the line of sight of 8–13 solar radii, frequency fluctuations of transmission radio signals were measured. During the experiments sharp increases in the variance of frequency fluctuations were recorded on both the eastern and western limbs. In measurements near the Earth's orbit on the Wind spacecraft in adjacent periods with a delay of 5–17 days, increases in the proton concentration and magnetic field strength were recorded at 7–15 times the background values. A comparison between the data related to the inner and near-Earth solar wind indicates that the observed disturbances are associated with the same region of the solar corona rotating with the Sun.

DOI: 10.1134/S0016793223600157

1. INTRODUCTION

It was found in (Efimov et al., 2019, 2020, 2021) that large-scale disturbances lead to an increase in frequency fluctuations of radio waves probing near-solar plasma. After this, after a time interval exceeding one-quarter of the rotation period of the Sun, a significant increase in the concentration of charged particles near the Earth's orbit is recorded, and after another quarter of a rotation, an increase in fluctuations is recorded when radio waves pass through the region located to the west of the Sun. Such a sequence of events is due to corotating large-scale disturbances that are formed by the interaction of slow and fast solar wind streams.

The purpose of this work, which is a continuation of (Efimov et al., 2019, 2020, 2021), was to study large-scale disturbances observed in the inner solar wind and near-Earth plasma in the period from August 18 to October 22, 2004. The probing radio waves were intensity variations (root mean square deviation) and the shapes of the time spectra of frequency fluctuations in the S- and X-bands.

2. CONDITIONS FOR CARRYING OUT RADIOSONDING OF NEAR- THE SUN PLASMA IN 2004

During 2004, long-term experiments were carried out on radio sounding of the near-solar plasma with decimeter (S-band, wavelength $\lambda_1 = 13.1$ cm) and centimeter (X-band, wavelength $\lambda_2 = 3.56$ cm) by Mars Express satellite signals. The geometric picture of radio sounding is illustrated Fig. 1, which shows the position of the projections of the spacecraft–Earth ray pathes onto the pattern plane for the Mars Express for each day of 2004. The horizontal axis shows the distances from the central meridian in units of the solar radius R_s, along the vertical axis are the distances from the equatorial plane. During the entire period from August 18 to October 22, 2004 the regions located to the north of the equator were sounded.

The geometric factors of radio sounding experiments are presented in Table 1, in which the dates of the experiments are also indicated in the form of days of the year. The closest approach of the ray path to the center of the Sun was reached on September 15, 2004 (DOY 259); it was $3.6R_s$ at the site of the sunset of the spacecraft and on September 16, 2004 (DOY 260), when the impact distance R was $3.85R_s$.

The investigated characteristics of the probing radio waves were the intensity (root mean square deviation) and the shape of the temporal spectra of frequency fluctuations in the S- and X-bands, as well as the differential frequency.

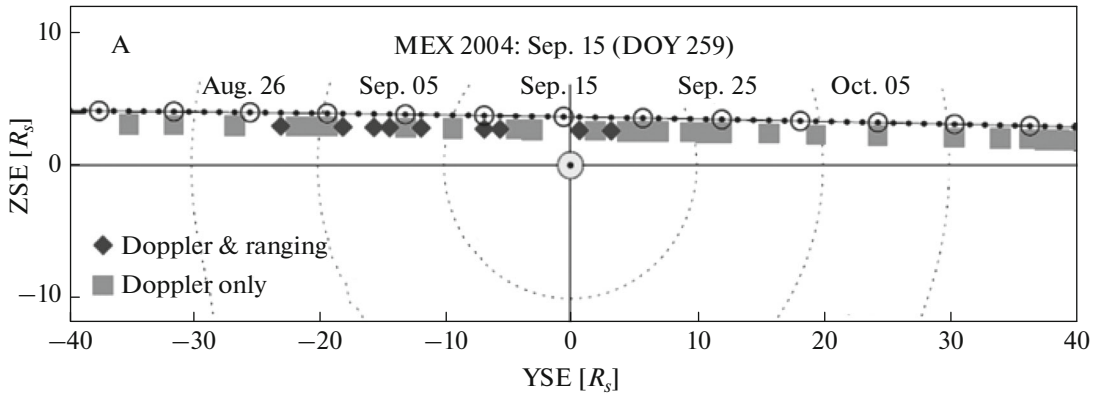

Fig. 1. The upper conjunction geometry as seen from Earth in the solar ecliptic coordinate system (Pätzold et al., 2012).

3. OBSERVATION OF DISTURBANCES IN NEAR THE SUN PLASMA IN RADIOSONDING EXPERIMENTS

During the preliminary processing of radio data obtained in experiments on probing the near-solar plasma with the signals of the Mars Express Mars satellite moving behind the Sun, two algorithms were used that complemented each other.

The first algorithm was used to determine the radial dependences of the intensity of S-band frequency fluctuations ($\lambda_1 = 13.1$ cm) and X-band ($\lambda_2 = 3.56$ cm). In Figure 2 the results of processing frequency fluctuations obtained at the phase of approach of the Mars Express spacecraft behind the solar disk and exit from behind it are presented (Efimov et al., 2013). The dark circles show the root-mean-square values of fluctuations of the frequency of the decimeter range σ_S, while the hollow circles are the similar characteristics for the centimeter range σ_X. Reduction of RMS values of frequency fluctuations of S- and X-band signals with an increasing impact distance R can be approximated by power functions of the form

$$\sigma_f = A_i(R/R_s)^{-m_i}, \quad (1)$$

where is the m-function exponent;

i is the S- or X-band;

R is the proximate distance of the radio path;

$R_s = 0.697 \times 10^6$ km is the radius of the Sun.

$$\left.\begin{array}{l} A_{\text{S in}} = 16.836 \text{ Hz} \quad m_{\text{S in}} = 1.90 \\ A_{\text{X in}} = 7.202 \text{ Hz} \quad m_{\text{X in}} = 1.87 \end{array}\right\} \text{at the site of the sunset of the spacecraft}$$

$$\left.\begin{array}{l} A_{\text{S egr}} = 20.712 \text{ Hz} \quad m_{\text{S egr}} = 1.91 \\ A_{\text{X egr}} = 8.340 \text{ Hz} \quad m_{\text{X egr}} = 1.86 \end{array}\right\} \text{at the site of the exit of the spacecraft from behind the Sun.}$$

the exponents m_S, m_X are close to each other, which indicates that the coronal structures on both sides of the Sun were similar and stable during the period from August 18 to October 22, 2004.

The second algorithm was used to search for temporal changes in the level of fluctuations of the differential frequency σ_D, which is a combination of S- and X-band frequencies and depends entirely on the characteristics of the plasma through which radio waves propagate (Pätzold et al., 2012). The studied characteristics in this case were the level of fluctuations of the differential frequency σ_D and variations of the integral

Table 1. The conditions for radio sounding of the near-sun plasma according to the signals of the *Mars Express* satellite in 2004

Days, 2004		Aiming distance, R/R_s	
sunset (Ingress)	exit	sunset (Ingress)	exit
231–259 August 18–September 15	260–296 September 16–October 22	32.20–3.60	3.85–46.74

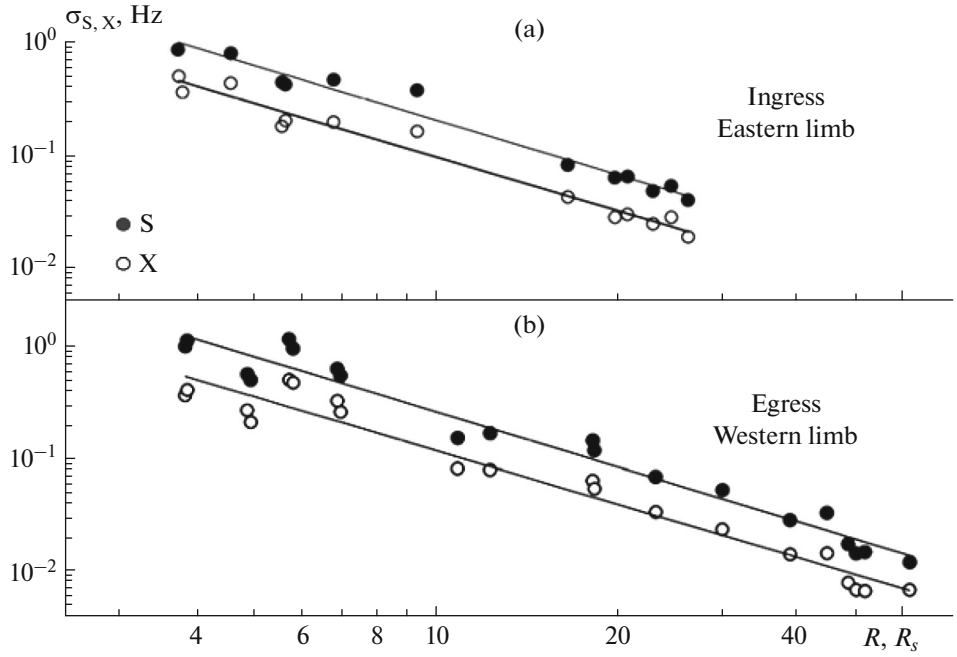

Fig. 2. The radial dependences of root-mean-square values of frequency fluctuations of S- and X-band signals according to the data of radio sounding experiments with the Mars Express spacecraft in 2004 (Efimov et al., 2013). (a), August 18–September 15, 2004; (b), September 17–October 22, 2004.

electron density ΔN_t plasma along the radio sounding path at the parts of the Mars Express spacecraft going behind the Sun (east limb) and at the exit from behind the Sun (west limb). The RMS values of the differential frequency σ_D taken from (Pätzold et al., 2012) are presented in Table 2 and Fig. 3 in the form of the dependencies σ_D from the proximate distance of the radio path R, expressed in units of the solar radius R_s.

Table 2. Fluctuations of the frequency difference (differential frequency) of the Mars Express satellite during radio sounding of circumsolar plasma in 2004

Eastern limb $\sigma_D = 16.683\ (R/R_s)^{-1.90}$				Western limb $\sigma_D = 20.712\ (R/R_s)^{-1.91}$			
Date 2004	DOY 2004	R/R_s	σ_f, Hz	Date 2004	DOY 2004	σ_f, Hz	R/R_s
Aug. 19.8	231.8	35.0	0.032	Sept. 15.0	259.0	0.706	3.9
Aug. 21.7	234.7	31.5	0.04	Sept. 17.5	261.5	1.42	4.7
Aug 26.0	239.0	26.0	0.054	Sept. 19.0	263.0	0.5	5.7
Aug 29.0	242.0	22.5	0.044	Sept. 19.6	263.6	1.42	6.3
Aug. 30.2	243.2	21.1	0.063	Sept. 20.6	264.6	0.6	7.45
Aug 30.8	243.8	20.3	0.056	Sept. 21.6	265.6	2.75	8.5
Aug 31.0	244.9	19.0	0.071	Sept. 23.0	267.0	0.167	10.6
Sept. 01.8	245.8	17.8	0.071	Sept. 24.2	268.2	0.183	12.0
Sept. 04.0	248.0	15.2	0.4	Sept. 25.2	269.2	0.348	13.1
Sept. 04.7	248.7	14.3	0.365	Sept. 28.2	272.2	0.125	16.7
Sept. 05.8	249.8	13.0	1.0	Oct. 01.3	275.3	0.083	20.4
Sept. 07.0	251.0	11.5	0.315	Oct. 06.2	280.2	0.057	26.2
Sept. 08.8	252.8	9.4	0.365	Oct 11.2	285.2	0.04	32.2
Sept. 10.7	252.8	7.0	0.5	Oct 16.3	290.3	0.035	38.0
Sept. 11.4	255.7	6.0	0.85	Oct 17.1	291.1	0.027	39.0
Sept. 12.0	256.0	5.3	0.795				
Sept. 13.6	257.6	4.3	1.62				

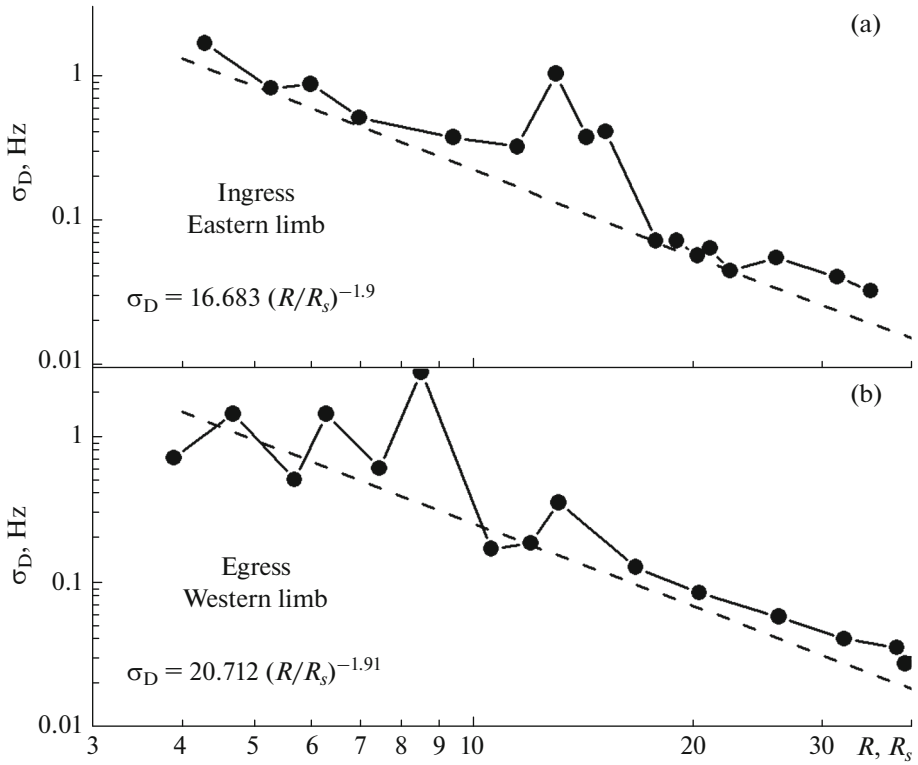

Fig. 3. The dependences of the variance of fluctuations of the differential frequency on the target distance of the radio beam when sounding the eastern region (a) and the western region (b) supercorona (Pätzold et al., 2012).

The dashed lines in Figs. 3 are the calculated dependencies $\sigma(R/R_s)$ following from relation (1) for frequency fluctuations of decimeter (S-band) radio waves. The values of σ_S are given in Table 3 for the proximate distances R/R_s = 4; 10; 20; 30; and 40 for the phase of the sunset of the spacecraft behind the Sun ($\sigma_{S\,in}$) and for the exit phase ($\sigma_{S\,egr}$). The measured statistical parameters of frequency fluctuations are proportional to the root-mean-square fluctuations of the plasma density and solar wind velocity near the proximate point of the line of sight.

Analysis of the presented data allows us to draw the following conclusions.

In most cases, the values of σ_D can be determined approximately on the basis of radial dependences obtained in the analysis of frequency variations in the decimeter wave range (1). The exceptions are the cases when the deviations from the mean dependencies $\sigma_S(R)$ exceed the measurement errors. Such cases need to be further analyzed. At the site where the spacecraft sets behind the Sun (eastern limb), such an event should be considered the observation of a sharp, almost by an order of magnitude, increase in the intensity of differential frequency fluctuations when the ray line passes at a distance $R = 13R_s$ from the center of the Sun. At the site of the exit of the spacecraft from behind the disk of the Sun (western limb), when the ray line is removed by a distance $R = 8.5R_s$ from its center, the level of fluctuations exceeds the expected value by more than 7 times. Another event recorded on the western limb may be located at the same distance as on the eastern $R = 13.1R_s$, but has a smaller amplitude: the measured value exceeds the expected value by ~2.5 times.

Obviously, these three events are associated with the manifestation of the specific structure of the solar supercorona.

Table 3. The calculated frequency fluctuation intensities of radio signals in the decimeter band during probing of the circumsolar plasma in August–October 2004

Aiming distance, R/R_s	4	10	20	30	40
$\sigma_{S\,in}$, Hz	1.27	0.22	0.055	0.0855	0.0150
σ_{Segr}, Hz	1.46	0.25	0.068	0.0310	0.0180

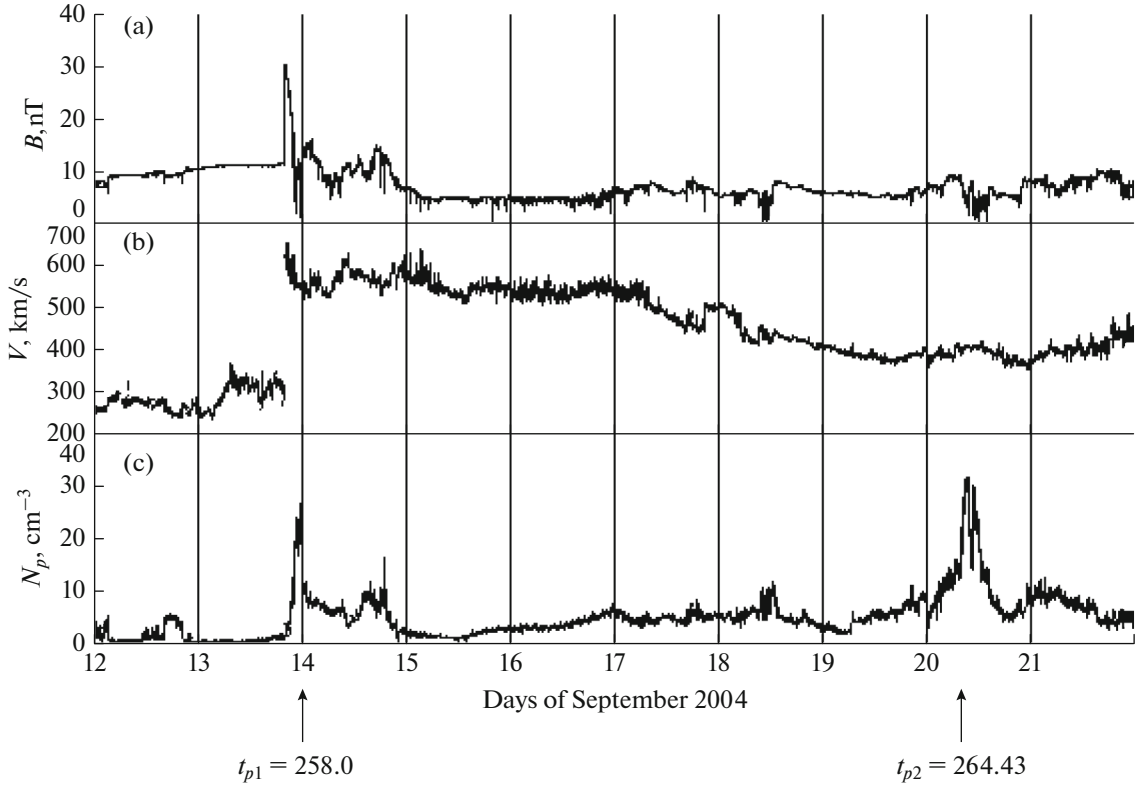

Fig. 4. The magnetic field induction dependences B (Fig. 4a), plasma flow velocities V (Fig. 4b), and proton concentration N_p (Fig. 4c) in the Earth's orbit according to Wind spacecraft data from September 12 to 21, 2004 (DOY 256–265).

4. OBSERVATION OF DISTURBANCES NEAR THE EARTH'S ORBIT IN THE PERIOD OF RADIO-SOUNDING EXPERIMENTS OF NEAR-SOLAR PLASMA

Figure 4 presents the results of measurements of plasma characteristics near the Earth's orbit at a moment of time, shifted relative to radio occultation observations by an interval equal to the time of motion of the solar wind plasma streams from the Sun to the Wind spacecraft.

The first event in the Earth's orbit was registered on September 14, 2004 (DOY 258) and was characterized by a significant increase in the magnetic field B at about 6 times the background value $B_f \approx 5$ nT (Fig. 4a) and the same increase in the proton concentration N_p (Fig. 4c). In the same period of time, increases in the velocity of plasma flows V were observed, first from 240 to 300 km/s, and then from 300 to 600 km/s (Fig. 4b).

The second event was recorded on September 20, 2004 (DOY 264.43) and consisted of a six-fold increase in the proton concentration. Other plasma characteristics (magnetic field B and velocity of plasma flows V) did not change significantly.

Table 1 allows one to reproduce the temporal dynamics of events that occurred during the experiments on radio sounding of circumsolar plasma using satellite signals of the Mars Express during the period from August 28 to September 22, 2004, and the phenomena in the Earth's orbit in adjacent time intervals recorded by the instruments of the Wind spacecraft. A graphical picture of these interconnected processes is presented in Fig. 5. The horizontal axis shows the days of 2004, the vertical axis shows the mean square values of σ_D observed on these dates of the fluctuations of the differential frequency of the signals from the Mars Express satellite that sounded the solar wind. The same axis indicates the times of observations of a sharp increase in the proton concentration in the Earth's orbit $t_{p1} = 258.0$ and $t_{p2} = 264.43$. The presented materials make it possible to trace the sequence of events near the Sun and in the vicinity of the Earth.

When the Mars Express satellite set behind the Sun, radio signals probed the supercorona regions located east of the center of the Sun from August 19 (DOY 231.84) to September 13 (DOY 257.6), 2004. The maximum fluctuations of the differential frequency $\sigma_{Dmax} = 1.00$ Hz was recorded on September 5, 2004 at the exact time $t_{p1} = 249.8$. The next event, a sharp increase in the concentration of protons, was recorded on September 14, 2004 (DOY 258). The third event was also observed near the Earth, the second time the concentration of protons increased by six times ($N_{p2} = 25$ cm^{-3}). The exact time of the second

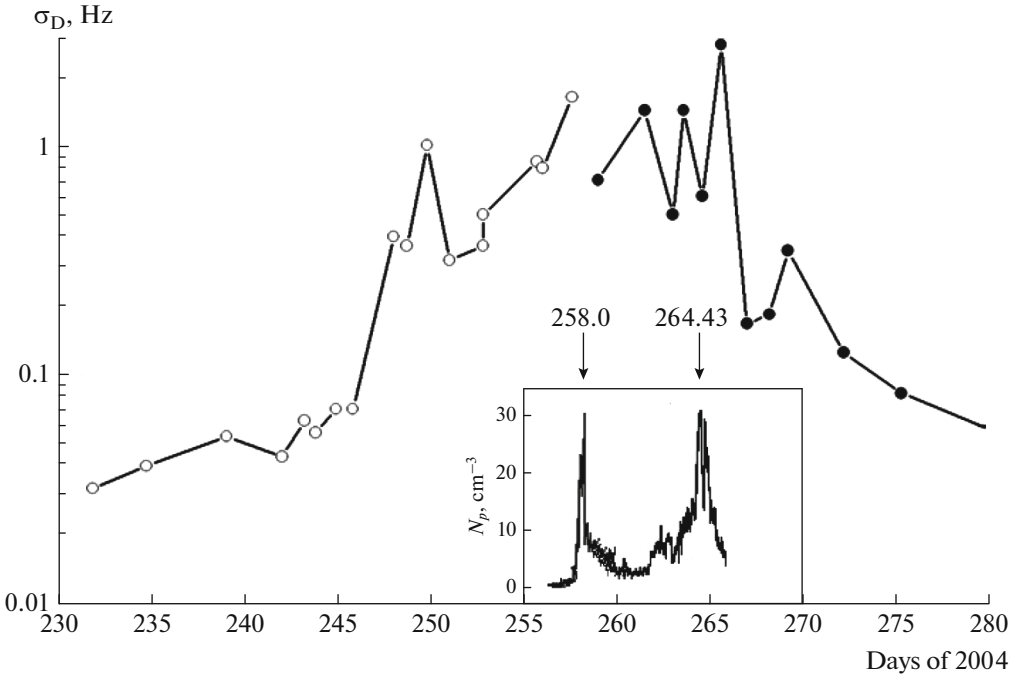

Fig. 5. The dispersion of the fluctuations of the differential frequency σ_D of the Mars Express signals during plasma probing on the eastern limb (light circles) and on the western limb (solid circles).

maximum on September 20, 2004 (t_{p2} = 264.43) differs from the time of the first maximum by 6.43 days, which is close to one-quarter of the solar rotation period (T = 27 days).

After the exit of the Mars Express from behind the disk of the Sun, radio signals probed regions of the supercorona located to the west of the center of the Sun. When the radio link is removed from the center of the Sun at a distance R = 8.35 solar radii R_s at UT = 1500 (DOY 265.625) a multiple increase in the fluctuations of the differential frequency of the radio waves that probed the circumsolar plasma is recorded. This event occurred 15.8 days after the generation of the disturbance on the eastern limb of the Sun (September 5, 2004, DOY 249.8) and 1 day (264.43) after the second proton concentration maximum near the Earth's orbit.

5. THE SEQUENCE OF DISTURBANCES

Eastern Limb–Near-Earth Plasma–Western Limb

It follows from Table 1 and Figs. 3 and 5 that on September 5, 2004 UT = 1400 (total time t = 249.8), when the Mars Express set behind the Sun on the eastern limb, an eight-fold increase in the intensity of differential frequency fluctuations was recorded. This event was associated with an increase in the electron density in the supercorona region, at a distance of $R = 13R_s$ from the center of the Sun and long-lived perturbations with an increased level of turbulence rotate with a period of ~T = 27 days. In this case, the plasma velocity is directed radially.

While the disturbance was observed on the eastern limb at the time t_0, the corresponding disturbance from the same region, which moved to the central meridian, reached the Earth's orbit at the time

$$t_0 + T/4 + \tau_2 = t_2,$$

where the second and third terms correspond to the turn from the east to the central meridian and propagation from the Sun to the Earth with an average velocity of V_2. This event manifests itself in the second increase in the proton concentration to

$$N_{p\ \max\ 2} = 30\ \text{cm}^{-3}.$$

In this case, the first increase in the plasma concentration in Fig. 4, DOY 258.0, is associated with the region of the solar corona that is ahead of the second maximum by about one-quarter of the period and was located near the central meridian near DOY 255. The two events are likely associated with different perturbed flows (sectoral structures), since they can be associated with the same large-scale disturbance only if its width in longitude exceeds 90°.

The region of increased concentration observed on the eastern limb due to the rotation of the Sun reaches the western limb at the time

$$t_3 = t_0 + T/2,$$

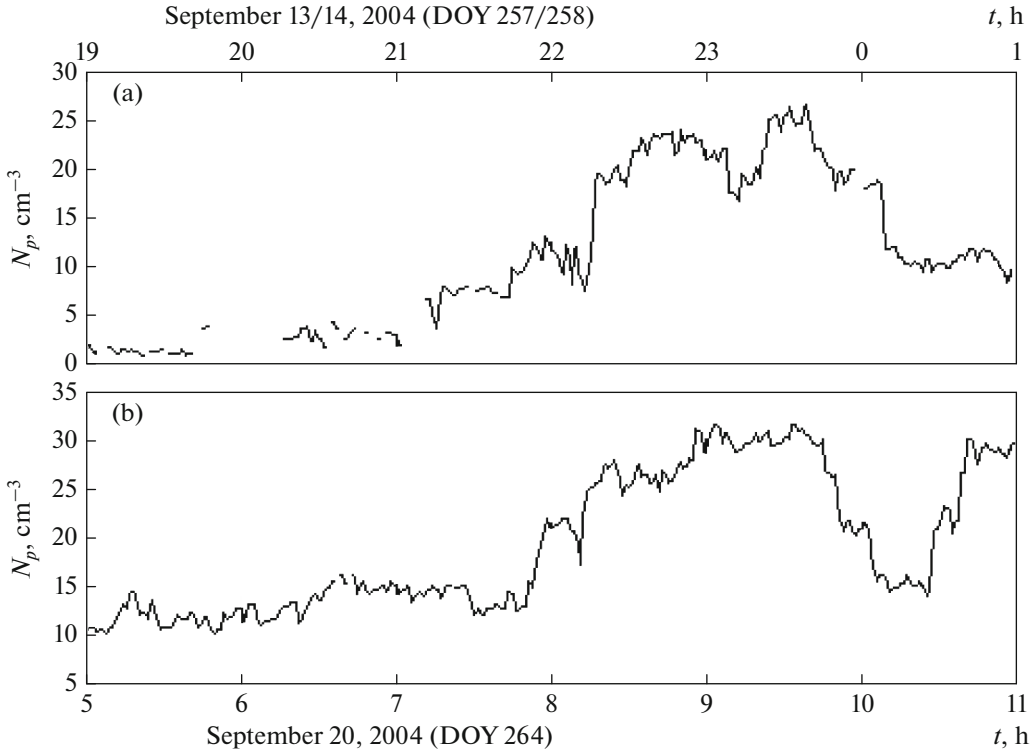

Fig. 6. The 1-minute values of the proton concentration N_p near the Earth's orbit according to the data of the Wind spacecraft during the experiments of radio sounding of the near-solar plasma with the signals of the Mars Express spacecraft in 2004. (a) DOY 257/258 (September 13/14) 2004, UT = 1900–0200. (b) DOY 264 (September 20) 2004, UT = 0500–1200.

which in the radio transmission data manifested itself in strong fluctuations of the differential frequency probing the solar supercorona at a distance $R = 8.5R_s$ according to the radio signals from the Mars Express.

In Figure 6 the 1-minute values of the proton concentration in the Earth's orbit are presented that were obtained in two measurement intervals aboard the Wind satellite completed between September 12 and September 21, 2004 (DOY 258–264). In these intervals, adjacent to the period of the radio sounding experiments of the near-solar plasma, the highest proton concentrations were recorded of $N_{p\ \max 1} = 25$ cm^{-3} and $N_{p\ \max 2} = 30$ cm^{-3}. The first measurement interval began on September 13, 2004, UT 1900, DOY 257 and ended on September 14, 2004, UT 0200, DOY 258 [Efimov et al., 2019, Fig. 6a]. It can be seen that higher N_p values were measured in the UT = 2140–0020 interval, i.e., during $\Delta t_1 = 2$ h 40 min. The maximum $N_{p\ \max 1}$ exceeded the background of $N_{01} = 5$ particles per cm^3 by 5 times. Similar values for the second measurement interval on September 20, 2004 were UT = 0800–1100, $\Delta t_2 = 3$ h 00 min, $N_{p\ \max 2}/N_{02} = 30/10 = 3$. It can be seen from Fig. 6 that the concentration time profiles for two disturbances separated by one-quarter of the period are qualitatively similar.

In Figure 7 the results of a comparison of measurements in 2004 performed in two regions of the heliosphere separated in space by a large distance (~1 AU) are presented. In Figure 7a changes in the integral electron density are shown during radio sounding of the circumsolar plasma according to the signals of the Mars Express as it set behind the Sun on September 5, 2004 (DOY 249, UT 1400–1700).

At that time, the radio communication line with the satellite of Mars passed through the regions of the supercorona located to the east of the Sun at an proximate distance $R = 13R_s$ (Pätzold et al., 2012). The horizontal axis shows the time of the experiment and frequency recording, the vertical axis shows the 1-minute values of the integral electron concentration in units of 10^{12} cm^{-2}. N_t during varied from 20–50 units (background value N_{t0}) up to ≈2200–2500 during the measurement time of $\Delta t_N = 3$ h.

In Figure 7b the 1-minute proton concentrations N_p are shown in the Earth's orbit, as measured by the *Wind* spacecraft on September 13 and 14, 2004 (DOY 257/258, UT 2200–0100). The maximum $N_{p\ \max} = 25$ cm^{-3} was reached on September 13, 2004 at UT 2340 and coincides with a similar maximum $N_{t\ \max}$ registered earlier on September 5, 2004 (DOY 249, UT 1540).

From Figure 7 it follows that the processes occurring in the vicinity of the Sun and in the Earth's orbit are similar to each other, but shifted in time. In fact,

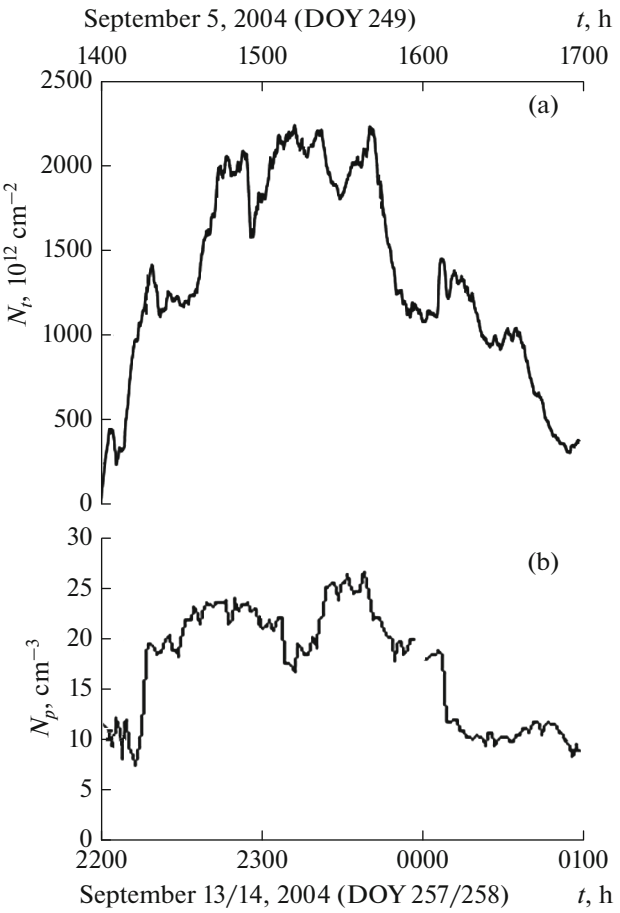

Fig. 7. (a), Changes in the integral electron concentration N_t during radio sounding on September 5, 2004 (DOY 249, UT 1400–1700) of the supercorona located to the east of the center of the Sun at an impact distance $R = 13R_s$ (Pätzold et al., 2012). (b), Changes in proton concentration N_p in Earth orbit according to the Wind spacecraft on September 13 and 14, 2004 (DOY 257/258, UT 2200–0100).

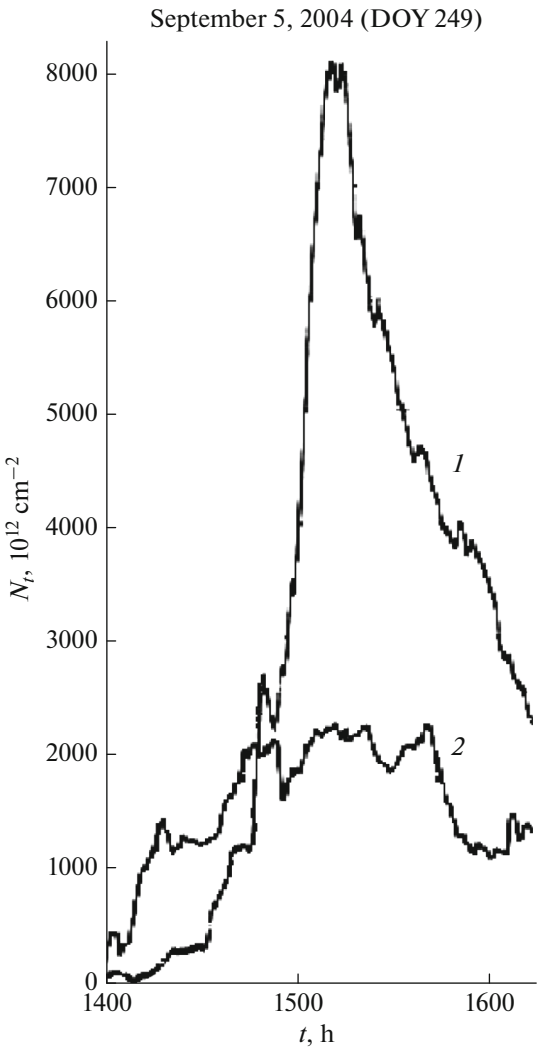

Fig. 8. Changes in the integral electron concentration N_t during radio sounding of the supercorona on the western limb at a distance of $8.5R_s$ (*1*) and on the eastern limb at a distance of $13R_s$ from the center of the sun (*2*).

the integral electron concentration N_t, and the proton density in the Earth's orbit differ from the background values only in the limited observation time interval, which is about 3 hours, exceeding the maximum values above the corresponding $N_{t\ \max}$ and $N_{p\ \max}$ background levels by ~3.5 times. The delay time of events in the Earth's orbit compared to the phenomena near the Sun is 8 days 8 hours, so that the speed of translation of processes from one region of the heliosphere to another is $V = 210$ km/s.

Thus, the previously obtained result (Efimov et al., 2021) was confirmed; when an increase in frequency fluctuations on the eastern limb is detected in radio sounding experiments it can be considered as a precursor of the arrival of SIR/CIR structures to the Earth with a lead time of 7.8 days.

Figure 8 presents the results of a comparison of the events that took place in 2004 in the regions of the supercorona located to the east of the center of the Sun at a heliocentric distance of $13R_s$ and west of the center at a closer distance of $8.5R_s$. It can be argued that in this case as well the duration of the perturbations is about 3 hours in both cases, and the maximum of the integral electron density $N_{t\ \max}$ increases strongly as the distance from the center of the Sun decreases from 2.2×10^{15} cm^{-2} at $R = 13R_s$ up to 8×10^{15} cm^{-2} at $R = 8.5R_s$. This is explained by a four-fold difference in the concentrations of charged particles.

6. CONCLUSIONS

Disturbances in the inner solar wind can be detected by continuous radio sounding of the solar wind with signals from radio sources of natural or artificial origins moving behind the Sun. The efficiency of

the study increases when monochromatic sounding sources are used, which have high stability in frequency and intensity. In the experiments of 2004, the studied characteristics were the frequency of signals from a Mars satellite moving behind the Sun, which probed the near-solar plasma, and the proton concentration near the Earth's orbit, measured by the instruments on the Wind spacecraft. Registration at the site of entry was carried out regularly from August 19 to September 13, 2004 (DOY 231–257) with a decrease in the sighting distance R from $35R_s$ up to $4.3R_s$. In this range of change in the impact distance, the intensity of fluctuations in the differential frequency is described by a power function (1). Increases in plasma density near the Earth's orbit occur after increases in frequency fluctuations on the eastern limb. disturbances on the western limb can be fixed after their registration near the Earth's orbit. In this case, the delay time in both cases is about one-quarter of the solar rotation period.

ACKNOWLEDGMENTS

The authors are grateful to M. Byrd and M. Petzold for providing data from radio sounding experiments.

FUNDING

The work was carried out within the framework of the State task.

CONFLICT OF INTEREST

The authors declare that they have no conflicts of interest.

REFERENCES

Efimov, A.I., Lukanina, L.A., Rudash, V.K., Samoznaev, L.N., Chashei, I.V., Bird, M.K., and Pätzold, M., Frequency fluctuations of coherent signals from spacecraft observed during dual-frequency radio sounding of the circumsolar plasma in 2004–2008, *Cosmic Res.*, 2013, vol. 51, no. 1, pp. 13–22.

Efimov, A.I., Lukanina, L.A., Smirnov, V.M., Chashei, I.V., Bird, M.K., and Pätzold, M., Disturbed flows in the inner solar wind and near Earth's orbit, *Cosmic Res.*, 2019, vol. 57, no. 6, pp. 423–433.

Efimov, A.I., Lukanina, L.A., Chashei, I.V., Kolomiets, S.F., Bird, M.K., and Pätzold, M., Observation of disturbed plasma structures in the environment of the Sun and near-Earth space with radio sounding and local measurements, *Cosmic Res.*, 2020, vol. 58, no. 6, pp. 460–467.

Efimov, A.I., Lukanina, L.A., Smirnov, V.M., Chashei, I.V., Bird, M.K., and Pätzold, M., Detection of strongly turbulent regions in the supercorona with the Venus Express and Mars Express satellites, *Geomagn. Aeron. (Engl. Transl.)*, 2021, vol. 61, no. 3, pp. 293–298.

Pätzold, M., Hahn, M., Tellmann, S., Häusler, B., Bird, M.K., Tyler, G.L., Asmar, S.W., and Tsurutani, B.T., Coronal density structures and CMEs: Superior solar conjunctions of *Mars Express, Venus Express*, and *Rosetta*: 2004, 2006, and 2008, *Sol. Phys.*, 2012, vol. 279, pp. 127–152.